Hindawi
Complexity
Volume 2019, Article ID 1507051, 9 pages
https://doi.org/10.1155/2019/1507051

Research Article

Neural Terminal Sliding-Mode Control for Uncertain Systems with Building Structure Vibration

Jianhui Wang,[1] **Wenli Chen**,[2] **Zicong Chen**,[2] **Yunchang Huang**,[2] **Xing Huang**,[1] **Wenqiang Wu**,[1] **Biaotao He**,[1] **and Chunliang Zhang**[1]

[1]*The School of Mechanical and Electric Engineering, Guangzhou University, Guangzhou 510006, China*
[2]*The School of Automation, Guangdong University of Technology, Guangzhou 510320, China*

Correspondence should be addressed to Wenqiang Wu; gz_wwq@gzhu.edu.cn and Chunliang Zhang; nhzcl@163.com

Received 29 October 2018; Revised 8 March 2019; Accepted 26 March 2019; Published 10 April 2019

Academic Editor: Yan-Ling Wei

Building structures occasionally suffer from unpredictable earthquakes, which can cause severe damage and can threaten human lives. Thus, effective control methods are needed to protect against structural vibration in buildings, and rapid finite-time convergence is a key performance indicator for vibration control systems. Rapid convergence can be ensured by applying a sliding-mode control method. However, this method would result in chattering issue, which would weaken the feasibility of the physical implementation. To address this problem, a neural terminal sliding-mode control method is proposed. The proposed method is combined with a terminal sliding-mode and a hyperbolic tangent function to ensure that the considered system can be stabilized in finite-time without chattering. Finally, the control effect of the proposed method is compared with that of LQR (linear quadratic regulator) control and switching function control. The simulation results showed that the proposed method can ensure rapid convergence while the chattering issue can be eliminated effectively. And the structural building vibration can be suppressed effectively too.

1. Introduction

Earthquakes are a natural phenomenon that can cause severe damage to building structures and can threaten human lives.Today, it remains difficult to predict when an earthquake may occur, and seismic waves are uncertain. Both factors pose challenges for building structure controllers during design. Thus, it is worth researching advanced antiseismic technology to protect building structures from vibration.

During the past few decades, many modern control methods, including linear quadratic regulator (LQR) control [1–3], sliding-mode control [4–6], and semiactive control [7–10], have proven active and effective measures in the area of structural vibration. These methods can stabilize the system. However, building structure vibrations cannot be effectively suppressed in finite-time, which might cause severe damage to the building structure.

To guarantee the rapid convergence of the system, sliding-mode control is applied for structural vibration control. According to the current deviation of the system and various derivative values, the vibration control method can change by jumping in the transient process. Therefore, the system can enter the sliding plane and obtain sliding-mode motion quickly, which ensures the rapid convergence of the system [11–14]. Meanwhile, the application of sliding-mode control is always accompanied by chattering, which may weaken the physical implementation rate.

By applying the hyperbolic tangent function, direct switching of the control input can be avoided, and chattering can be eliminated. This approach allows the system to respond to the outside world in a timely manner and facilitates physical implementation. However, most control methods use Lyapunov stability, which belongs to the field of asymptotic stability research; in this field, the stable time goes toward infinity, which is meaningless for the control of structural vibrations [15–19].

As research on the combination of Lyapunov stability theory and the theorem of homogeneity has developed, finite-time stable control methods have progressed. Finite-time stable control has been widely applied, for example, in the

position control of synchronous permanent magnet motors and in high-precision guidance laws [20–23]. However, the finite-time stable control method is rarely applied to structural vibrations.

However, uncertainties that could affect system stability exist in practical systems. The guarantee of finite-time stability when considering a system with uncertainty is an outstanding research area. Neural networks can be used to approximate any nonlinear function with generalization. Thus, a Radial Basis Function (RBF) neural network is adopted to address this problem; see [24–28].

The neural terminal sliding-mode control method is proposed in this work to address an uncertain system with structural vibrations. An RBF neural network is combined with a terminal sliding-mode and the hyperbolic tangent function to handle an uncertain system with structural vibrations. The finite-time stabilization method is used to stabilize the building structural system in finite-time. As shown below, the main compensatory mechanism and contributions of the proposed schemes are summarized as follows.

Most traditional control methods were researched without considering uncertainty and rapid convergence performance, which may result in serious damage to building structures [3–5]. Rapid convergence can be ensured by applying a sliding-mode control method; however, uncertainty affects rapid convergence, which poses a considerable challenge regarding controller design. Thus, a combination of a RBF neural network and terminal sliding-mode control is proposed to solve the uncertainty issues and ensure rapid convergence.

In practice, chattering weakens the feasibility of physical implementation, which means that stable timeliness cannot be guaranteed and substantial structural damage may occur [8–10]; therefore, the feasibility of physical applications is important to determine. In this paper, finite-time control is combined with a hyperbolic tangent function to eliminate chattering and prevent structural building vibrations in finite time.

The remainder of this paper is organized as follows. In Section 2, models and a problem formulation are proposed. Then, the neural terminal sliding-mode control method is proposed to address the uncertain system with structural vibrations. In Section 3, the control effect of the proposed method is compared with the LQR control method and switching function control. The simulation results showed that the proposed method can effectively eliminate chattering, ensure rapid convergence, and effectively suppress structural building vibration. Finally, conclusions are given in Section 4.

2. Modeling and Analysis of Building Structures

2.1. Modeling Building Structures under Earthquake Conditions. A building structure optimized for interlaminar shear is used for modeling. Thus, the n-layer building structure can be simplified as a building structure with n degrees of freedom. Under earthquake conditions, the dynamic equation can be described as follows:

$$\mathrm{M}\ddot{D} + C\dot{D} + KD = F\ddot{x}_g + \mathrm{Q}U \tag{1}$$

where $D = [d_1, d_2, d_3, ..., d_n]^{\mathrm{T}}$ is the displacement vector of the structure, $d_i (i = 1, 2, ..., n)$ is the displacement of the ith floor (relative to the ground) of the building structure, K is the stiffness matrix, M is the mass matrix, $F = -MI$ is the transformation matrix of the ground seismic acceleration, where $I = \begin{bmatrix} 1 & 1 & \cdots & 1 \end{bmatrix}^{\mathrm{T}}$ is the unit column of $n \times 1$, C is the damping matrix, $\ddot{x}_g$ is the ground seismic acceleration, Q is a matrix denoting the location of the actuators, and U is the control input.

Defining a state-space vector

$$\mathrm{Y} = \left[y_1, y_2\right]^T \tag{2}$$

where $\mathrm{y}_1 = [y_{11}, y_{12}, \ldots, y_{1n}]^T = D$ and $y_2 = [y_{21}, y_{22}, ..., y_{2n}]^T = \dot{D}$. Equation (1) is rewritten as follows:

$$\dot{\mathrm{Y}} = A_r \mathrm{Y} + W_r \ddot{x}_g + B_r U \tag{3}$$

where $A_r = \begin{bmatrix} 0 & I_{n\times n} \\ -M^{-1}K & -M^{-1}C \end{bmatrix}$, $W_r = \begin{bmatrix} 0 \\ M^{-1}F \end{bmatrix}$, $B_r = \begin{bmatrix} 0 \\ M^{-1}\mathrm{Q} \end{bmatrix}$.

According to the rank criterion, the controllability of the building structure under earthquake conditions can be certified. Thus, structural vibration can be restrained by designing a control variable setting as follows:

$$U = \mathrm{Q}^{-1}\left(C\dot{D} + KD + \mathrm{M}V\right) \tag{4}$$

where $V = [u_1, u_2, ..., u_n]^T$ is a variable derived from (2) and (3) as follows:

$$\dot{\mathrm{Y}} = \begin{bmatrix} 0 & I_{n\times n} \\ 0 & 0 \end{bmatrix} \mathrm{Y} + \begin{bmatrix} 0 \\ I_{n\times n} \end{bmatrix} \left(V - M^{-1}\mathrm{F}\ddot{x}_g\right) \tag{5}$$

Setting $f = -\ddot{x}_g$, the system is composed of a mutually independent subsystem, which is described as follows:

$$\begin{aligned} \dot{y}_{11} &= y_{21} \\ \dot{y}_{21} &= u_1 - f \\ \dot{y}_{12} &= y_{22} \\ \dot{y}_{22} &= u_2 - f \\ &\cdots \\ \dot{y}_{1n} &= y_{2n} \\ \dot{y}_{2n} &= u_n - f \end{aligned} \tag{6}$$

The seismic wave is uncertain. Thus, further analysis is difficult. Neural finite-time stable control is used to handle this problem.

2.2. Approximation System Research. Analyzing the system above, seismic wave $\ddot{x}_g$ is assumed to be known. The RBF neural network is chosen to approximate $\ddot{x}_g$ because it can effectively approximate the unknown variable [29]. The network algorithm is designed as follows:

$$h_j = \exp\left(-\frac{\left\|x - c_j\right\|^2}{2b_j^2}\right) \tag{7}$$

$$f = W^{*T} h(x) + \varepsilon \tag{8}$$

where x is an input of the network, j is the jth joint of the hidden-layer of the network, $h = [h_1, \cdots, h_j, \cdots h_N]^T$, $N \geq 0$, and W^* is the desirable permission of the network, ε is the approximate error of the network, and $\varepsilon \leq \varepsilon_N$. According to the above analysis, the model can be described as follows:

$$\begin{aligned} f(y) &= W^{*T} h(\mathrm{y}) \\ \widehat{f}(\mathrm{y}) &= \widehat{W}^T h(\mathrm{y}) \end{aligned} \tag{9}$$

Because function f is unknown, to offset the effect of function f on the system, the RBF neural network is used to approximate the function, which allows (4) to be rewritten as follows:

$$U = \mathrm{Q}^{-1}\left(C\dot{D} + K\dot{D} + \mathrm{M}V + \mathrm{F}\widehat{f}\right) \tag{10}$$

2.3. Terminal Sliding-Mode Controller Design. u_i is the ith controller, and y_{1i}, y_{2i} denotes the displacement of the ith floor (relative to the ground) of the building structure. Thus, the structural building model with uncertain earthquakes can be described as follows:

$$\begin{aligned} \dot{y}_{1i} &= y_{2i} \\ \dot{y}_{2i} &= -\widetilde{f} + u_i \end{aligned} \tag{11}$$

Remark 1. f is the actual seismic wave, and $\widehat{f}$ is the estimated value approximated by RBF; therefore, $\widetilde{f}$ is the error of the actual value and the estimated value. Thus, $\widetilde{f} = f - \widehat{f}$.

The sliding-mode function is designed as follows:

$$s = P(\mathrm{E} - Z) \tag{12}$$

where $e = y_{1i} - y_{1di}$, $\dot{e} = y_{2i} - y_{2di}$, $P = [p, 1]$, $\mathrm{E} = x - x_d = \left[e \;\; \dot{\mathrm{e}}\right]^T$, and $Z = \left[z(t) \;\; \dot{z}(t)\right]^T$. Thus, we can obtain

$$s = p\mathrm{e} - pz(t) + \dot{\mathrm{e}} - \dot{z}(t) \tag{13}$$

where p must satisfy the Hurwitz condition ($p > 0$).

Remark 2. For Y of the system to track desired state $[y_{1di}, y_{2di}]$ within appointed time T, [30] proposes a method of constructing terminal function $Z(t)$. The method is designed as follows.

To achieve global robustness, $E(0) = Z(0)$, i.e., $e(0) = z(0), \dot{e}(0) = \dot{z}(0)$. To achieve the convergence of appointed time T, $z(t) = 0, \dot{z}(t) = 0, \ddot{z}(t) = 0$. Therefore, the terminal function can be described as follows:

$$z(t) = \begin{cases} e(0) + \dot{e}(0)t + \frac{1}{2}\ddot{e}(0)t^2 - \left(\frac{b_{00}}{T^3}e(0) + \frac{b_{01}}{T^2}\dot{e}(0) + \frac{b_{02}}{T}\ddot{e}(0)\right)t^3 + \left(\frac{b_{10}}{T^4}e(0) + \frac{b_{11}}{T^3}\dot{e}(0) + \frac{b_{12}}{T^2}\ddot{e}(0)\right)t^4 - \left(\frac{b_{20}}{T^5}e(0) + \frac{b_{21}}{T^4}\dot{e}(0) + \frac{b_{22}}{T^3}\ddot{e}(0)\right)t^5 & 0 \leq \mathrm{t} \leq \mathrm{T} \\ 0, & t \geq T \end{cases} \tag{14}$$

where b_{ij} $(i, j = 0, 1, 2)$ is a coefficient that can be obtained by solving the equation.

The derivative of (13) can be obtained as follows:

$$\dot{s} = p\dot{e} - p\dot{z}(t) + \ddot{e} - \ddot{z}(t) \tag{15}$$

If $\ddot{e} = \dot{\mathrm{y}}_{2i} - \dot{y}_{2d} = -\widetilde{f} + u - \dot{y}_{2d}$, then

$$\dot{s} = p\dot{e} - p\dot{z}(t) - \widetilde{f} + u - \dot{y}_{2d} - \ddot{z}(t) \tag{16}$$

Remark 3. The hyperbolic tangent function is as follows:

$$\tanh\left(\frac{x}{\varepsilon}\right) = \frac{e^{x/\varepsilon} - e^{-x/\varepsilon}}{e^{x/\varepsilon} + e^{-x/\varepsilon}} \tag{17}$$

where $\varepsilon > 0$ and the speed of the inflection point of the hyperbolic tangent smooth function depends on the value of ε.

The controller is designed as follows:

$$u = -p\dot{e} + p\dot{z}(t) + \dot{y}_{2d} + \ddot{z}(t) - \eta \tanh\left(\frac{s}{\varepsilon}\right) \tag{18}$$

where η is a positive design parameter.

Derived from (16) and (18):

$$\dot{s} = -\widetilde{f} - \eta \tanh\left(\frac{s}{\varepsilon}\right) \tag{19}$$

A Lyapunov function is defined as follows:

$$V = \frac{1}{2}s^2 + \frac{1}{2\lambda}\widetilde{W}^T\widetilde{W} \tag{20}$$

Then, the derivative of (20) can be obtained as follows:

$$\dot{V} = s\dot{s} - \frac{1}{\lambda}\widetilde{W}^T\dot{\widehat{W}} \tag{21}$$

2.4. Stability Analysis. Derived from (21):

$$\begin{aligned} \dot{V} &= s\left(-\widetilde{f} - \eta \tanh\left(\frac{s}{\varepsilon}\right)\right) - \frac{1}{\lambda}\widetilde{W}^T\dot{\widehat{W}} \\ &= -s\eta \tanh\left(\frac{s}{\varepsilon}\right) - s\widetilde{f} - \frac{1}{\lambda}\widetilde{W}^T\dot{\widehat{W}} \end{aligned}$$

$$= -s\eta \tanh\left(\frac{s}{\varepsilon}\right) - s\widetilde{W}h - \frac{1}{\lambda}\widetilde{W}^T\dot{\widehat{W}}$$
$$= -s\eta \tanh\left(\frac{s}{\varepsilon}\right) - \widetilde{W}\left(sh + \frac{\dot{\widehat{W}}}{\lambda}\right) \tag{22}$$

Lemma 4 (see [31]). *For any given x, $\varepsilon > 0$ and there is an inequality:*

$$x \tanh\left(\frac{x}{\varepsilon}\right) = \left|x \tanh\left(\frac{x}{\varepsilon}\right)\right| = |x| \left|\tanh\left(\frac{x}{\varepsilon}\right)\right| \geq 0 \tag{23}$$

The explanation for Lemma 4 is as follows.

According to the definition of the hyperbolic tangent function, we have the following:

$$x \tanh\left(\frac{x}{\varepsilon}\right) = x\frac{e^{x/\varepsilon} - e^{-x/\varepsilon}}{e^{x/\varepsilon} + e^{-x/\varepsilon}} = \frac{1}{e^{2(x/\varepsilon)} - 1} x\left(e^{2(x/\varepsilon)} - 1\right) \tag{24}$$

Thus, it can be said that

$$\begin{aligned} \mathrm{e}^{2(x/\varepsilon)} - 1 \geq 0, \quad x \geq 0 \\ e^{2(x/\varepsilon)} - 1 < 0, \quad x < 0 \end{aligned} \tag{25}$$

Hence,

$$x\left(\mathrm{e}^{2(x/\varepsilon)} - 1\right) \geq 0 \tag{26}$$

Then,

$$x \tanh\left(\frac{x}{\varepsilon}\right) = \frac{1}{\mathrm{e}^{2(x/\varepsilon)} + 1} x\left(\mathrm{e}^{2(x/\varepsilon)} - 1\right) \geq 0 \tag{27}$$

Thus, the consequence can be achieved such that

$$x \tanh\left(\frac{x}{\varepsilon}\right) = \left|x \tanh\left(\frac{x}{\varepsilon}\right)\right| = |x| \left|\tanh\left(\frac{x}{\varepsilon}\right)\right| \geq 0 \tag{28}$$

which completes the proof.

Setting $sh = \dot{\widehat{W}}/\lambda$, so $\dot{\widehat{W}} = -\lambda sh$:

$$\dot{V} = -s\eta \tanh\left(\frac{s}{\varepsilon}\right) \leq 0 \tag{29}$$

From the above discussion, system stability can be proven.

From the expression of function $\mathrm{Z}(t)$, when $t = 0$, $\mathrm{z}(0) = e(0)$ and $\dot{z}(0) = \dot{e}(0)$ (i.e., $s(0) = P(\mathrm{E}(0) - \mathrm{Z}(0)) = 0$). Hence, the initial system state is already on the sliding surface, which eliminates the arrival phase of the sliding film and ensures the global robustness and stability of the closed-loop system.

Remark 5. Because the system has global robustness, i.e., $\mathrm{E}(t) = Z(t)$, design function $Z(T) = 0$ can be used to ensure that $\mathrm{E}(T) = 0$ so that the tracking error converges to zero within finite time T.

To achieve convergence for a specified time T, it is necessary to ensure that when $t = T$, $z(T) = 0$, $\dot{z}(T) = 0$ and $\ddot{z}(T) = 0$, where $\ddot{z}(T) = 0$ meets the requirements of (14). Therefore, when $0 \leq t \leq T$, function $z(t)$ and its derivative can be written as follows:

$$\begin{aligned} z(t) = {} & e(0) + \dot{e}(0)t + \frac{1}{2}\ddot{e}(0)t^2 \\ & - \left(\frac{b_{00}}{T^3}e(0) + \frac{b_{01}}{T^2}\dot{e}(0) + \frac{b_{02}}{T}\ddot{e}(0)\right)t^3 \\ & - \left(\frac{b_{10}}{T^4}e(0) + \frac{b_{11}}{T^3}\dot{e}(0) + \frac{b_{12}}{T^2}\ddot{e}(0)\right)t^4 \\ & - \left(\frac{b_{20}}{T^5}e(0) + \frac{b_{21}}{T^4}\dot{e}(0) + \frac{b_{22}}{T^3}\ddot{e}(0)\right)t^5 \end{aligned} \tag{30}$$

The derivative of (30) is as follows:

$$\begin{aligned} \dot{z}(t) = {} & \dot{\mathrm{e}}(0) + \ddot{e}(0)t \\ & + 3\left(\frac{b_{00}}{T^3}e(0) + \frac{b_{01}}{T^2}\dot{\mathrm{e}}(0) + \frac{b_{02}}{T}\ddot{e}(0)\right)t^2 \\ & + 4\left(\frac{b_{10}}{T^4}e(0) + \frac{b_{11}}{T^3}\dot{\mathrm{e}}(0) + \frac{b_{12}}{T^2}\ddot{e}(0)\right)t^3 \\ & + 5\left(\frac{b_{20}}{T^5}e(0) + \frac{b_{21}}{T^4}\dot{\mathrm{e}}(0) + \frac{b_{22}}{T^3}\ddot{e}(0)\right)t^4 \end{aligned} \tag{31}$$

The derivative of (31) is as follows:

$$\begin{aligned} \ddot{z}(t) = {} & \ddot{e}(0) + 6\left(\frac{b_{00}}{T^3}e(0) + \frac{b_{01}}{T^2}\dot{e}(0) + \frac{b_{02}}{T}\ddot{e}(0)\right)t \\ & + 12\left(\frac{b_{10}}{T^4}e(0) + \frac{b_{11}}{T^3}\dot{e}(0) + \frac{b_{12}}{T^2}\ddot{e}(0)\right)t^2 \\ & + 20\left(\frac{b_{20}}{T^5}e(0) + \frac{b_{21}}{T^4}\dot{e}(0) + \frac{b_{22}}{T^3}\ddot{e}(0)\right)t^3 \end{aligned} \tag{32}$$

When $t = T$, we can obtain $z(T) = 0$. Thus,

$$\begin{aligned} z(T) = {} & \mathrm{e}(0) + \dot{e}(0)T + \frac{1}{2}\ddot{e}(0)T^2 \\ & + \left(\frac{b_{00}}{T^3}e(0) + \frac{b_{01}}{T^2}\dot{e}(0) + \frac{b_{02}}{T}\ddot{e}(0)\right)t^3 \\ & + \left(\frac{b_{10}}{T^4}e(0) + \frac{b_{11}}{T^3}\dot{e}(0) + \frac{b_{12}}{T^2}\ddot{e}(0)\right)t^4 \\ & + \left(\frac{b_{20}}{T^5}e(0) + \frac{b_{21}}{T^4}\dot{e}(0) + \frac{b_{22}}{T^3}\ddot{e}(0)\right)t^5 \\ = {} & \left(1 + b_{00} + b_{10} + b_{20}\right)e(0) \\ & + T\left(1 + b_{01} + b_{11} + b_{21}\right)\dot{e}(0) \\ & + T^2\left(\frac{1}{2} + b_{02} + b_{12} + b_{22}\right)\ddot{e}(0) = 0 \end{aligned} \tag{33}$$

The necessary conditions for the establishment of $z(T) = 0$ are as follows:

$$\begin{aligned} 1 + b_{00} + b_{10} + b_{20} &= 0 \\ 1 + b_{01} + b_{11} + b_{21} &= 0 \\ 0.5 + b_{02} + b_{12} + b_{22} &= 0 \end{aligned} \tag{34}$$

Similarly, when $t = T$, the necessary condition for $\dot{z}(T) = 0, \ddot{z}(T) = 0$ is as follows:

$$\begin{aligned} 3b_{00} + 4b_{10} + 5b_{20} &= 0 \\ 1 + 3b_{01} + 4b_{11} + 5b_{21} &= 0 \\ 1 + 3b_{02} + 4b_{12} + 5b_{22} &= 0 \end{aligned} \tag{35}$$

$$\begin{aligned} 6b_{00} + 12b_{10} + 20b_{20} &= 0 \\ 6b_{01} + 12b_{11} + 20b_{21} &= 0 \\ 1 + 6b_{02} + 12b_{12} + 20b_{22} &= 0 \end{aligned} \tag{36}$$

Three ternary equations can be sorted by the above equations:

$$\begin{aligned} b_{00} + b_{10} + b_{20} &= -1 \\ 3b_{00} + 4b_{10} + 5b_{20} &= 0 \\ 6b_{00} + 12b_{10} + 20b_{20} &= 0 \end{aligned} \tag{37}$$

$$\begin{aligned} b_{01} + b_{11} + b_{21} &= -1 \\ 3b_{01} + 4b_{11} + 5b_{21} &= -1 \\ 6b_{01} + 12b_{11} + 20b_{21} &= 0 \end{aligned} \tag{38}$$

$$\begin{aligned} b_{02} + b_{12} + b_{22} &= -0.5 \\ 3b_{02} + 4b_{12} + 5b_{22} &= -1 \\ 6b_{02} + 12b_{12} + 20b_{22} &= -1 \end{aligned} \tag{39}$$

According to $\mathrm{B}x = G$, to express the ternary equations, the above three equations can be written as the following three forms:

$$\mathrm{B}_1 x_1 = G_1,$$

$$\mathrm{B}_1 = \begin{bmatrix} 1 & 1 & 1 \\ 3 & 4 & 5 \\ 6 & 12 & 20 \end{bmatrix}, \quad \mathrm{G}_1 = \begin{bmatrix} -1 \\ 0 \\ 0 \end{bmatrix} \tag{40}$$

$$\mathrm{B}_2 x_2 = G_2,$$

$$\mathrm{B}_2 = \begin{bmatrix} 1 & 1 & 1 \\ 3 & 4 & 5 \\ 6 & 12 & 20 \end{bmatrix}, \quad \mathrm{G}_2 = \begin{bmatrix} -1 \\ -1 \\ 0 \end{bmatrix} \tag{41}$$

$$\mathrm{B}_3 x_3 = G_3,$$

$$\mathrm{B}_3 = \begin{bmatrix} 1 & 1 & 1 \\ 3 & 4 & 5 \\ 6 & 12 & 20 \end{bmatrix}, \quad \mathrm{G}_3 = \begin{bmatrix} -0.5 \\ -1 \\ -1 \end{bmatrix} \tag{42}$$

The solution to the above equations is as follows:

$$\begin{aligned} b_{00} &= -10 \\ b_{10} &= 15 \\ b_{20} &= -6 \\ b_{01} &= -6 \\ b_{11} &= 8 \\ b_{21} &= -3 \\ b_{02} &= -1.5 \\ b_{12} &= 1.5 \\ b_{22} &= -0.5 \end{aligned} \tag{43}$$

Moreover, through further solutions:

$$z(t) = \begin{cases} \mathrm{e}(0) + \dot{\mathrm{e}}(0)t + \frac{1}{2}\ddot{\mathrm{e}}(0)t^2 - \left(\frac{10}{T^3}\mathrm{e}(0) + \frac{6}{T^2}\dot{\mathrm{e}}(0) + \frac{3}{2T}\ddot{\mathrm{e}}(0)\right)t^3 + \left(\frac{15}{T^4}\mathrm{e}(0) + \frac{8}{T^3}\dot{\mathrm{e}}(0) + \frac{3}{2T^2}\ddot{\mathrm{e}}(0)\right)t^4 - \left(\frac{6}{T^5}\mathrm{e}(0) + \frac{3}{T^4}\dot{\mathrm{e}}(0) + \frac{1}{2T^3}\ddot{\mathrm{e}}(0)\right)t^5 & 0 \le \mathrm{t} \le \mathrm{T} \\ 0, & t > T \end{cases} \tag{44}$$

where L_∞ is defined as a finite function set.

Remark 6. From (30), we know $\dot{V} \leq 0$, which means that Lyapunov function $V(t)$ must be nonincreasing with respect to the time variable. Because the initial value $V(0)$ is finite, it follows that $V(t) \in L_\infty$. Thus, $V(t)$ is bounded, which allows us to obtain the following:

$$\lim_{t \longrightarrow \infty} V(t) = 0 \tag{45}$$

Derived from (21), it is determined that s and $\widetilde{W}$ are bounded.

Because $s = P(\mathrm{E} - Z)$ and the closed-loop system enters the sliding stage at the initial moment, we can determine that $s(0) = 0$, i.e., $\mathrm{E}(t) \equiv Z(t)$. Because s is bounded and P is a constant, Z(t) can converge within finite time T, and E(t) can converge within finite time T. Therefore, according to the preset terminal function Z(t), the output error can be guaranteed to converge to zero within a finite time to ensure the system can be stabilized within a finite time.

3. Control Method Analysis

In this section, three control methods were simulated: LQR control, switching function control, and neural terminal sliding-mode finite-time stable control. Based on a three-layer building structure, the system is subjected to an El earthquake wave. The maximum earthquake acceleration is $\mathrm{a}_{\max} = 3.417 m/s^2$. The parameters of the proposed control are set as $p = 1$, $\mathrm{T} = 1$, and $\varepsilon = 0.02$. The mass matrix, damping matrix, stiffness matrix, and the position of the examples are set as follows:

$$\begin{aligned} M &= 10^4 \times \begin{bmatrix} 3.456 & 0 & 0 \\ 0 & 3.456 & 0 \\ 0 & 0 & 3.456 \end{bmatrix} (kg) \\ C &= 10^5 \times \begin{bmatrix} 1.745 & -0.512 & -0.111 \\ -0.512 & 1.634 & -0.623 \\ -0.111 & -0.623 & 1.122 \end{bmatrix} (Ns/m) \\ K &= 10^6 \times \begin{bmatrix} 2.4 & -1.2 & 0 \\ -1.2 & 2.4 & -1.2 \\ 0 & -1.2 & 1.2 \end{bmatrix} (N/m) \\ Q &= \begin{bmatrix} 1 & 0 & 0 \\ 0 & 1 & 0 \\ 0 & 0 & 1 \end{bmatrix} \end{aligned} \tag{46}$$

Example 1. No control, LQR control, and proposed control for the three-layer building structure are simulated. The contrast simulation curves of displacement, velocity, acceleration response, and control force are shown in Figures 1–4.

According to Table 1, the LQR control compared with no control, the maximum displacement of the first, second, and third floors decreased by 59.9%, 67.6%, and 71.9%, respectively. And the maximum velocity decreased by 34.3%, 46%, and 46.4%, respectively. Meanwhile, the proposed control method compared with no control, the maximum displacement of the first, second, and third floors decreased by 97.1%, 98.4%, and 98.7%, respectively. And the maximum velocity decreased by 92.6%, 94.8%, and 94.6%, and maximum acceleration decreased by 64.7%, 56.5%, and 54.5%, respectively.

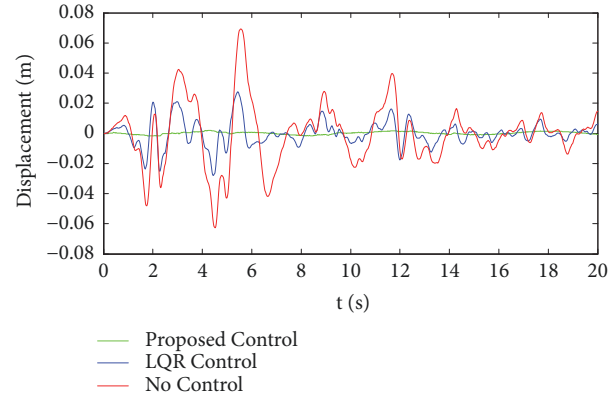

Figure 1: Displacement response of Example 1.

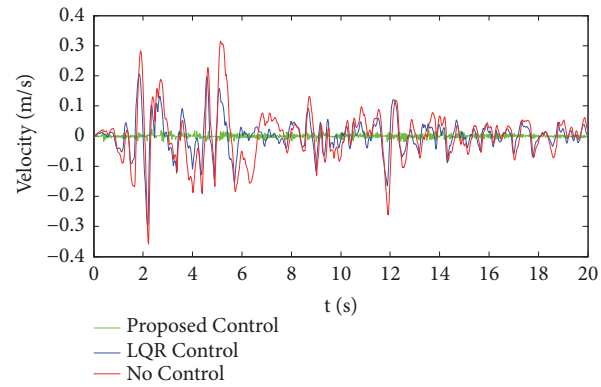

Figure 2: Velocity response of Example 1.

Example 2. In Example 2, two control methods, i.e., switch control and the proposed control, are simulated for the three-layer building structure. Contrast simulation curves of displacement, velocity, acceleration response, and control force are shown in Figures 5–8, respectively.

According to Table 2, the switch control compared with no control, the maximum displacement of the first, second, and third floors decreased by 78%, 88%, and 90.4%, respectively. The maximum velocity decreased by 84.3%, 88.9%, and 88.6%, respectively, and maximum acceleration decreased by 77.9%, 72.7%, and 71.5%, respectively. Meanwhile, the proposed method compared with no control, the maximum displacement of the first, second, and third floors decreased by 97.1%, 98.4%, and 98.7%, respectively. The maximum velocity decreased by 26.1%, 47.6%, and 46.1%, respectively. And maximum acceleration decreased by 64.7%, 56.5%, and 54.5%, respectively.

Table 1: Maximum displacement, velocity, and acceleration of in Example 1.

Control Strategy Parameter		Proposed Control	LQR Control	No Control
Displacement (mm)	First floor	2	27.7	69.2
	Second floor	2	41.1	127
	Third floor	2	44.6	159
Velocity (m/s)	First floor	0.023	0.206	0.314
	Second floor	0.023	0.239	0.443
	Third floor	0.023	0.231	0.431
Acceleration (m/s^2)	First floor	1.7019	4.92	4.82
	Second floor	1.7019	4.00	3.91
	Third floor	1.7019	3.71	3.74

Table 2: Maximum displacement, velocity, and acceleration of Example 2.

Control Strategy Parameter		Proposed Control	Switch Control	No Control
Displacement (mm)	First floor	2	15.2	69.2
	Second floor	2	15.2	127
	Third floor	2	15.2	159
Velocity (m/s)	First floor	0.0232	0.049	0.314
	Second floor	0.0232	0.049	0.443
	Third floor	0.0232	0.049	0.431
Acceleration (m/s^2)	First floor	1.7019	1.065	4.82
	Second floor	1.7019	1.065	3.91
	Third floor	1.7019	1.065	3.74

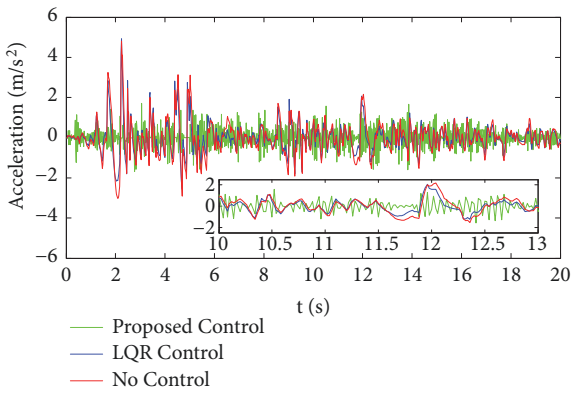

Figure 3: Acceleration response of Example 1.

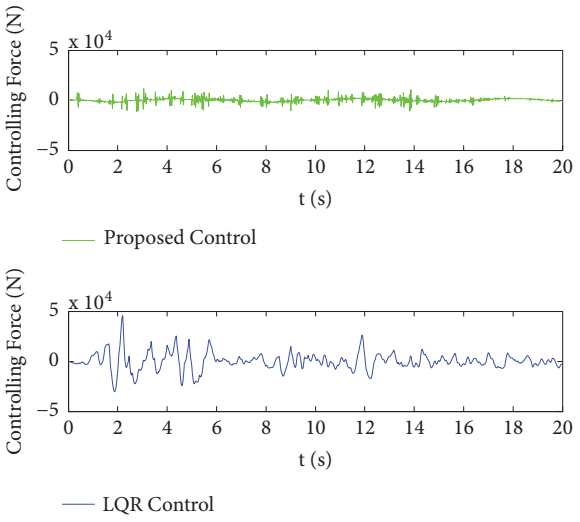

Figure 4: Controlling force of Example 1.

Meanwhile, Figure 8 clearly shows that strong chattering exists when using the switching function control force, which cannot be removed with these methods.

From Figure 9, we could know that El Center Acceleration can be approximated by the adopted RBF neural networks effectively. Then, according to the two examples above, both switching function control and the proposed control methods effectively restrain structural vibration. Then, considering practical applications, strong chattering can be effectively resolved by the proposed control method. And the displacements of three-layer buildings can be bounded within a small range. Furthermore, displacement, velocity, and acceleration could tend toward a small range of vibration and stabilize. Therefore, a neural terminal sliding-mode finite-time stable control algorithm can better protect the building structure from earthquake damage and effectively reduce the buffering problem in sliding-mode control.

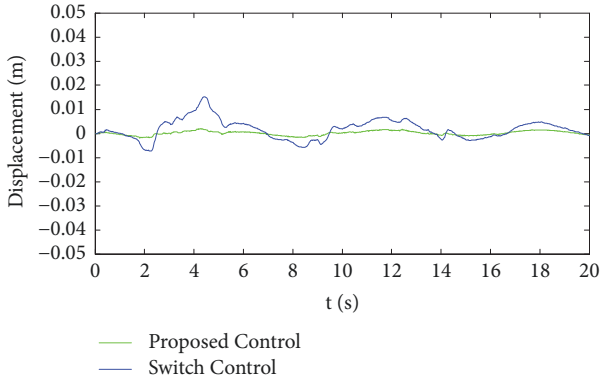

Figure 5: Displacement response of Example 2.

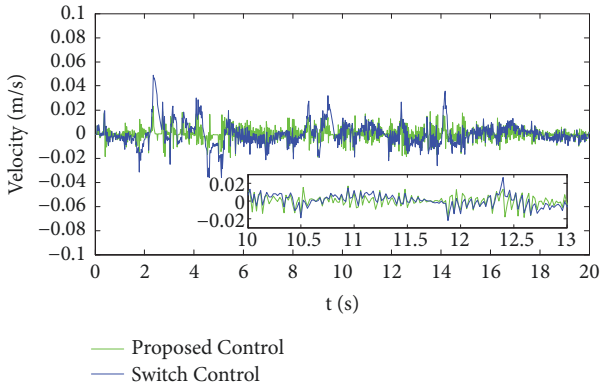

Figure 6: Velocity response of Example 2.

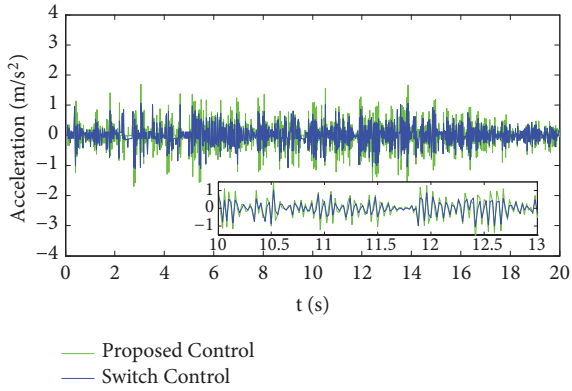

Figure 7: Acceleration response of Example 2.

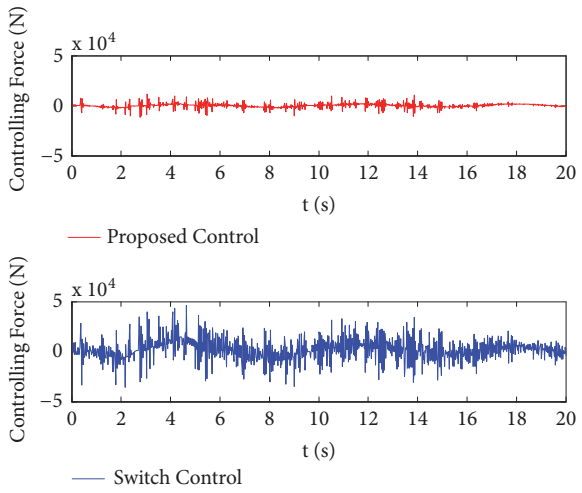

Figure 8: Controlling force of Example 2.

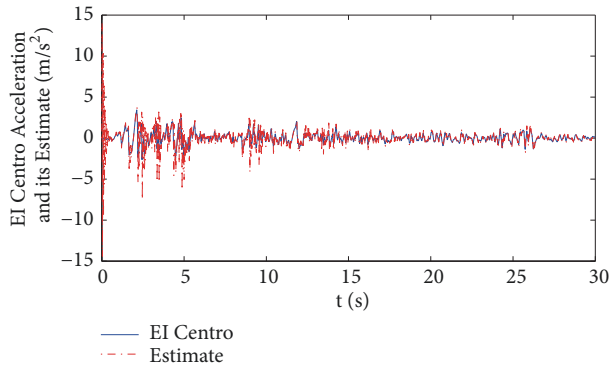

Figure 9: El Center Acceleration and its estimate.

4. Conclusion

In this paper, neural terminal sliding-mode control for uncertain systems subject to structural building vibration is proposed. Uncertainties are typically challenging when striving to ensure rapid convergence for controller design, which has been solved by combining an RBF neural network with terminal sliding-mode control. The traditional sliding-mode control inevitably causes chattering problems, which result in considerable challenges regarding physical implementation. Furthermore, it is important to ensure sliding-mode control without chattering issues. Thus, a hyperbolic tangent function is used to design the controller, allowing the stability of the system to be demonstrated. Finally, the control effect of the neural terminal sliding-mode finite-time stable control method is compared with the LQR control and switching function control methods. The feasibility and effectiveness of the proposed methods are verified. However, the input constraints of actual system require further research.

Data Availability

The structural building data used to support the findings of this study are included within the article.

Conflicts of Interest

The authors declare that there are no conflicts of interest regarding the publication of this paper.

Acknowledgments

This work is supported by the National Natural Science Foundation (NNSF) of China (Grant Numbers 51775122 and

51505092), the Guangzhou City College Scientific Research Project (Grant Number 1201630173), the Science and Technology Planning Project of Guangdong (Grant Number 2016B090912007), the Natural Science Foundation of Guangdong Province, China (Grant Number 2015A030308011), and the Program of the Foshan Innovation Team of Science and Technology (Grant Number 2015IT100072).

References

[1] T. Yong, S. S. Chen, and Q. Y. Tu, "Approaches to structural vibration control for civil engineering," *Construction & Design for Project*, vol. 8, pp. 1007–9467, 2011.

[2] S. L. Wang, W. Liu, and T. Yang, "Experimental study on vibration control of Xiaoyan Pagoda in Xian," *Journal of Vibration and Shock*, vol. 16, pp. 1000–3835, 2017.

[3] Y. Kong, "Isolation vibration reduction and vibration control analysis of building structures," *Architectural knowledge*, vol. 15, pp. 1002–8544, 2017.

[4] Y. Zhou, C. C. Hu, G. X. Zhou et al., "Study on shake table model design method affliction pendulum isolated structures," *Structural Engineering International*, vol. 5, pp. 6–11, 2015.

[5] J. H. Wang, Z. Liu, C. Chen, and Y. Zhang, "Fuzzy adaptive compensation control of uncertain stochastic nonlinear systems with actuator failures and input hysteresis," *IEEE Transactions on Cybernetics*, vol. 49, pp. 2–13, 2019.

[6] X. L. Lu, *Seismic Theory of Complex High-Rise Buildings with Application*, Science Press, Beijing, China, 2nd edition, 2015.

[7] C. Q. Zhang, X. L. Lu, J. B. Li et al., "The research of the seismic performance of a multi-tower structure," *Structural Engineers*, 1, pp. 123–127, 2011.

[8] Y. S. Li, C. Z. Xiao, L. F. Jin et al., "Displacement analysis and control study on support of high-rise structures connected with high corridor," *China Civil Engineering Journal*, vol. 12, pp. 1–8, 2013.

[9] Z. J. Zhao, X. Y. He, Z. G. Ren, and G. L. Wen, "Boundary adaptive robust control of a flexible riser system with input nonlinearities," *IEEE Transactions on Systems, Man, and Cybernetics: Systems*, 2018, in press.

[10] Z. J. Zhao, X. Y. He, Z. G. Ren, and G. L. Wen, "Output feedback stabilization for an axially moving system," *IEEE Transactions on Systems, Man, and Cybernetics: Systems*, 2018, in press.

[11] J.-M. Wang, J.-J. Liu, B. Ren, and J. Chen, "Sliding mode control to stabilization of cascaded heat PDE-ODE systems subject to boundary control matched disturbance," *Automatica*, vol. 52, pp. 23–34, 2015.

[12] Z. Q. Li and K. Wang, "Chattering-free of sliding-mode control applied to structural vibration," *Computer Engineering and Applications*, vol. 11, pp. 229–232, 2017.

[13] J. Yao, "Research on chattering elimination of sliding mode variable structure," *Mechanical & Electrical Engineering Technology*, vol. 9, pp. 1009–9492, 2016.

[14] Z. Chen, G. Wen, H. Zhou, and J. Chen, "Generation of grid multi-scroll chaotic attractors via hyperbolic tangent function series," *Optik - International Journal for Light and Electron Optics*, vol. 130, pp. 594–600, 2017.

[15] Can He, Jianchun Xing, Juelong Li, Qiliang Yang, and Ronghao Wang, "A New Wavelet Thresholding Function Based on Hyperbolic Tangent Function," *Mathematical Problems in Engineering*, vol. 2015, Article ID 528656, 10 pages, 2015.

[16] Z. J. Liu, Z. J. Zhao, and C. K. Ahn, "Boundary constrained control of flexible string systems subject to disturbances," *IEEE Transactions on Circuits and Systems II*, 2019, in press.

[17] Y. Wei, J. H. Park, J. Qiu, L. Wu, and H. Y. Jung, "Sliding mode control for semi-Markovian jump systems via output feedback," *Automatica*, vol. 81, pp. 133–141, 2017.

[18] S. K. S. Fan and T. Y. Lee, *Using Hyperbolic Tangent Function for Nonlinear Profile Monitoring*, Springer, Singapore, 2013.

[19] Z.-x. Chen and F.-l. Cao, "The construction and approximation of feedforward neural network with hyperbolic tangent function," *Applied Mathematics-A Journal of Chinese Universities Series B*, vol. 30, no. 2, pp. 151–162, 2015.

[20] C. S. Kenney and A. J. Laub, "A hyperbolic tangent identity and the geometry of Padé sign function iterations," *Numerical Algorithms*, vol. 7, no. 2-4, pp. 111–128, 1994.

[21] J. H. Wang, H. Y. Zhu, C. L. Zhang et al., "Adaptive Hyperbolic Tangent Sliding-mode Control for Building Structural Vibration Systems for Uncertain Earthquakes," *IEEE Access*, vol. 6, pp. 74728–74736, 2018.

[22] M. M. Polycarpou and P. A. Ioannou, "A robust adaptive nonlinear control design," in *Proceedings of the IEEE American Control Conference*, pp. 1365–1369, 1993.

[23] P. A. Ioannou and J. Sun, *Robust Adaptive Control*, PTR Prentice-Hall, 1996.

[24] Y. Wei, J. Qiu, P. Shi, and L. Wu, "A piecewise-markovian lyapunov approach to reliable output feedback control for fuzzy-affine systems with time-delays and actuator faults," *IEEE Transactions on Cybernetics*, vol. PP, no. 99, pp. 1–13, 2017.

[25] X. Gao, Y. Chen, D. You, Z. Xiao, and X. Chen, "Detection of micro gap weld joint by using magneto-optical imaging and Kalman filtering compensated with RBF neural network," *Mechanical Systems and Signal Processing*, vol. 84, pp. 570–583, 2017.

[26] H. Mirinejad and T. Inanc, "An RBF collocation method for solving optimal control problems," *Robotics and Autonomous Systems*, vol. 87, pp. 219–225, 2017.

[27] S. Ding and X. H. Chang, "Simulation study of function approximation performance based on gaussian-RBF neural networks," *Hennan Science*, vol. 31, pp. 1383–1386, 2013.

[28] R. Ma, S. Qiu, Q. Jiang et al., "AI-2 quorum sensing negatively regulates rbf expression and biofilm formation in Staphylococcus aureus," *International Journal of Medical Microbiology*, vol. 307, no. 4-5, pp. 257–267, 2017.

[29] C. Yang, X. Wang, and Z. Li, "Teleoperation control based on combination of wave variable and neural networks," *IEEE Transactions on Systems Man & Cybernetics Systems*, vol. 99, pp. 1–12, 2017.

[30] K. Y. Zhuang, K. Q. Zhang, H. Y. Su, and etc., "Terminal sliding mode control for high-order nonlinear dynamic systems," *Journal of Zhejiang University (Engineering Science)*, no. 36, pp. 482–539, 2002.

[31] M. P. Aghababa and M. E. Akbari, "A chattering-free robust adaptive sliding mode controller for synchronization of two different chaotic systems with unknown uncertainties and external disturbances," *Applied Mathematics and Computation*, vol. 218, no. 9, pp. 5757–5768, 2012.